Supporting Information

Emergence of Long Afterglow and Room Temperature Phosphorescence Emission from Ultra Small Sulfur Dots

Karthika S Sunil[1#], Kommula Bramhaiah[1#], Srayee Mandal[1], Subhajit Kar[1], Neena S John[2], and Santanu Bhattacharyya[1*]

[1]Indian Institute of Science Education and Research Transit Campus, Govt. ITI Building (transit campus), Engg. School Road, Berhampur, Odisha-760010 (India)

[2]Centre for Nano and Soft Matter Sciences (CeNS), Arkavathi Campus, Survey No.7, Shivanapura, Dasanapura Hobli, Bangalore – 562162 (India)

E-mail: santanub@iiserbpr.ac.in

#-Equal Contributions
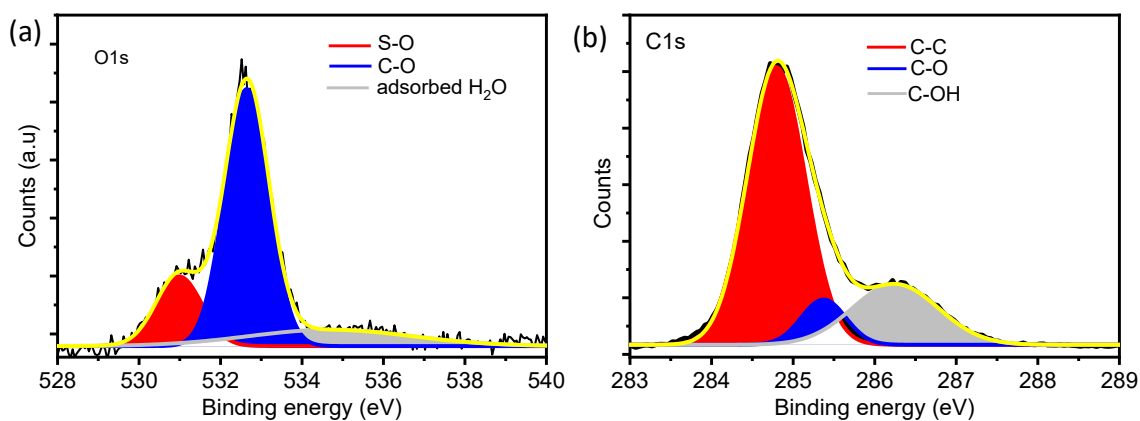
Figure S1. Deconvoluted (a) O1s and (b) C1s spectra of as-synthesized S-dots employing mechanical grinding assisted approach.
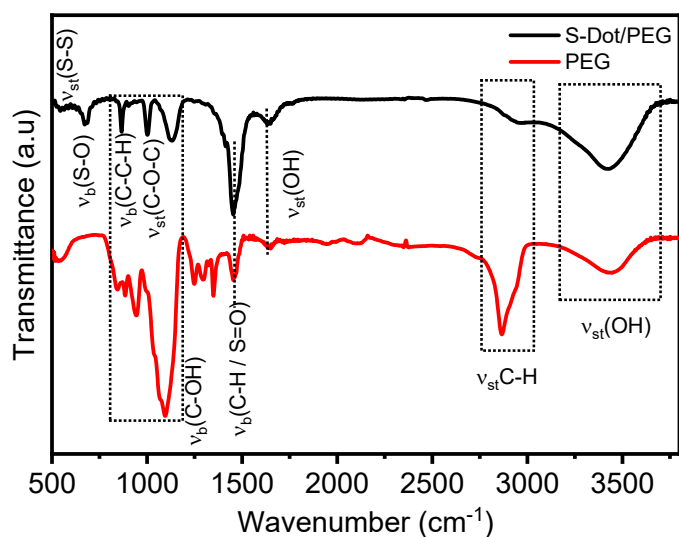
Figure S2. FTIR spectra of S-dots synthesized employing mechanical grinding assisted synthesis approach and PEG molecules.
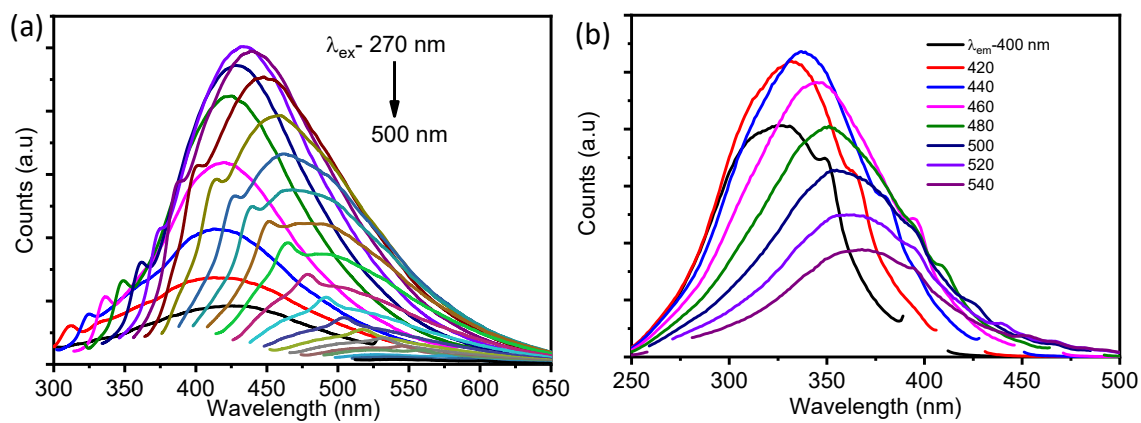
Figure S3. (a) Fluorescence emission spectra with λ_{ex} of 270 nm to 500 nm with increasing 10 nm (b) fluorescence excitation spectra at various emission wavelengths of S-dots.
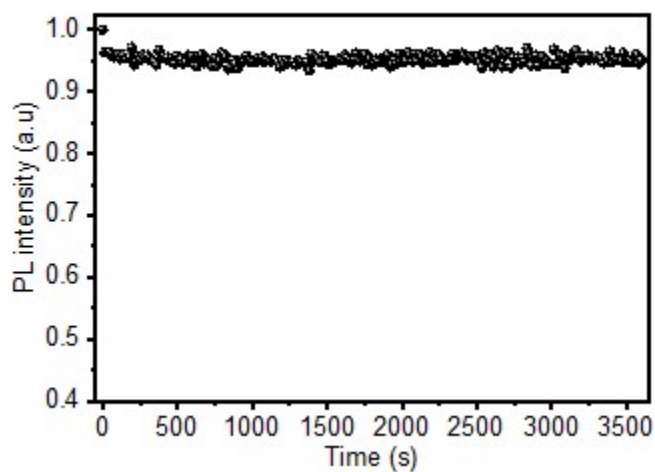
Figure S4. Fluorescence stability plot of S-dots.
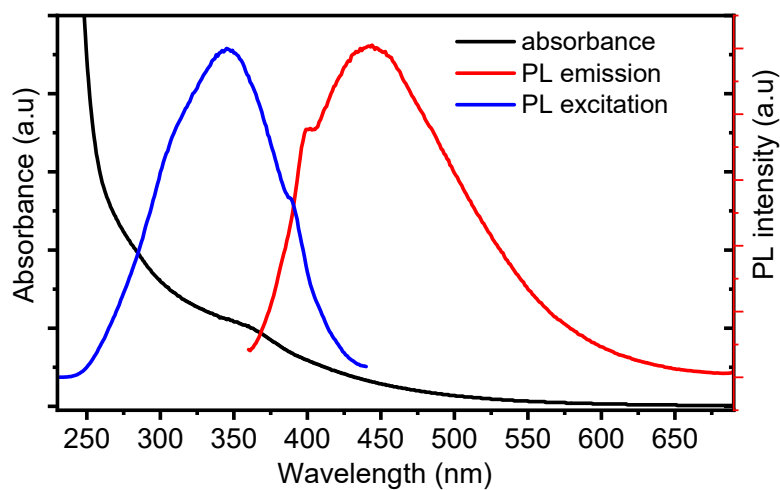
Figure S5. Absorbance, PL emission, and PL excitation spectra of S-dots synthesized employing mechanical grinding approach after 3 months.

Table S1. Time-resolved lifetime data of as-synthesized S-dots employing a mechanical grinding approach at various excitation wavelengths.

Sample	λ_{ex} (nm)	A_1	τ_1 (ns)	A_2	τ_2 (ns)	$<\tau>$ (ns)
	340	0.80	1.72	0.20	8.33	3.04
S-dots	375	0.76	0.41	0.24	3.46	1.14
	450	0.79	0.13	0.21	2.74	0.68
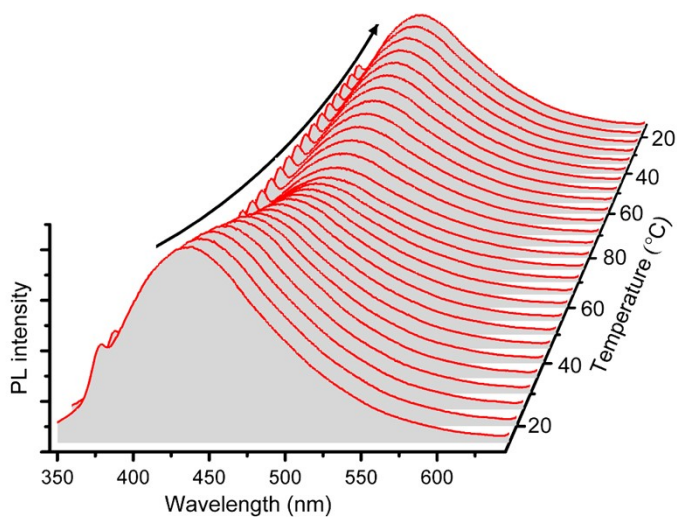
Figure S6. Thermo-responsive PL spectra of S-dots by varying the temperature from 15 °C to 80 °C, and 80 °C to 15 °C; heating and cooling processes, respectively.
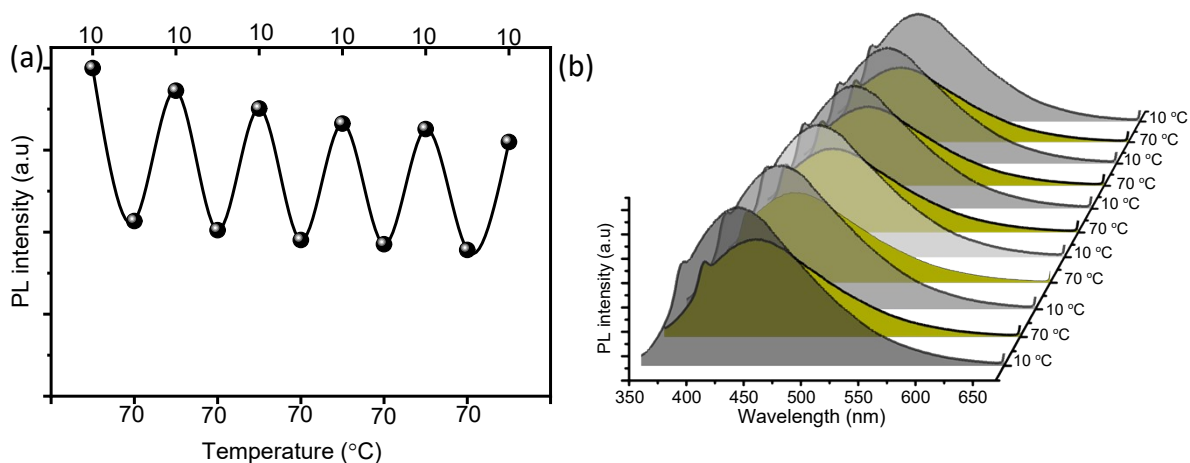
Figure S7. (a) Plot of PL intensity versus temperature (b) PL emission spectra of S-dots at various cooling (10 °C) and heating (10 °C) cycles for the as-synthesized employing mechanical grinding approach.
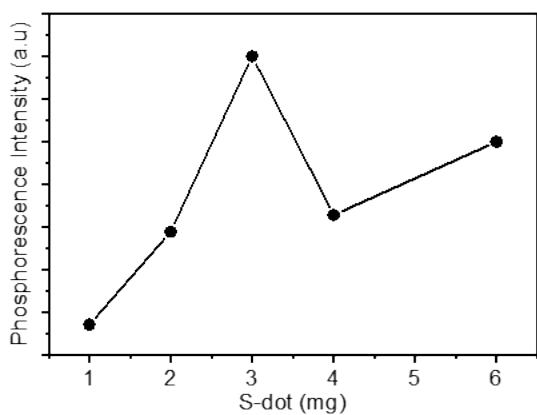
Figure S8. phosphorescence intensity by varying the S-dot (wt) in the boron oxide matrix.
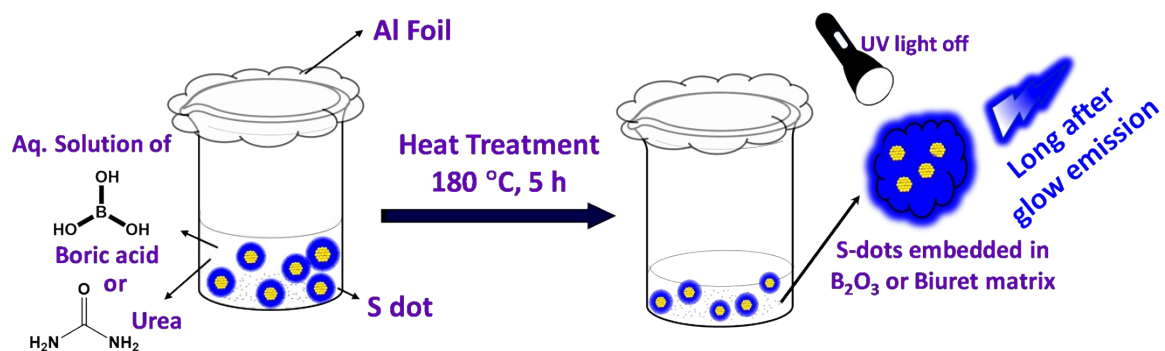
Figure S9. Schematic representation of synthesis process for the S-dots-B_2O_3 composite and S-dots-biuret composite.
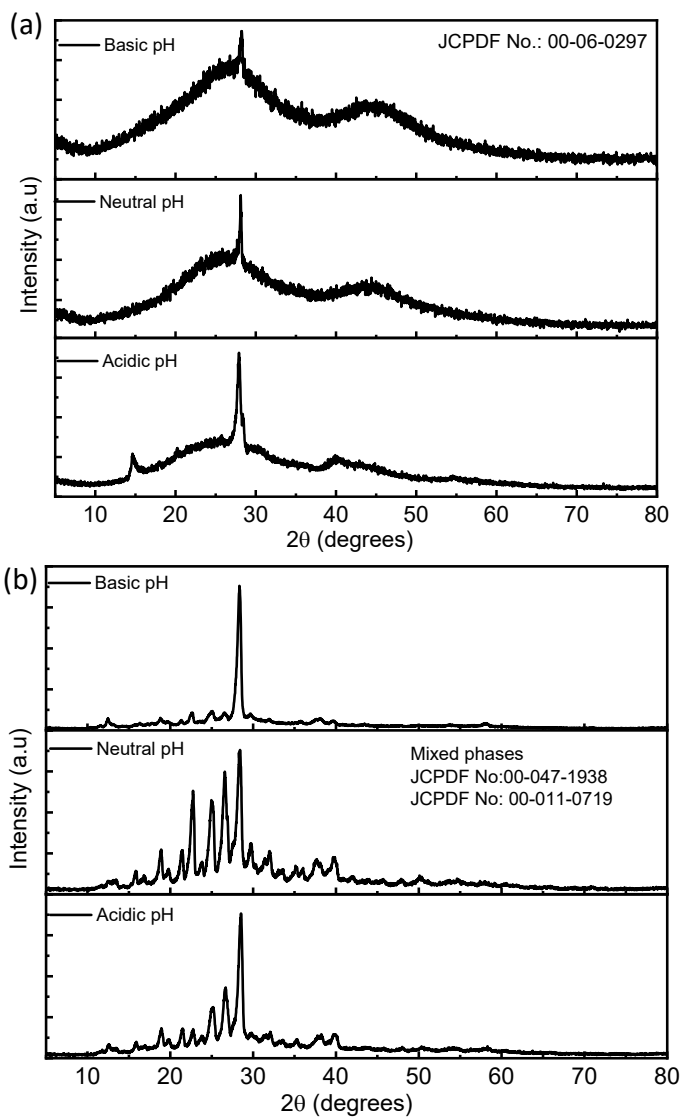
Figure S10. XRD spectra of S-dots embedded in various matrixes such as boron oxide and biuret matrix (a) S-dots in boron oxide matrix at various pH (acidic, neutral, and basic) (b) S-dots in biuret matrix at various pH (acidic, neutral, and basic).
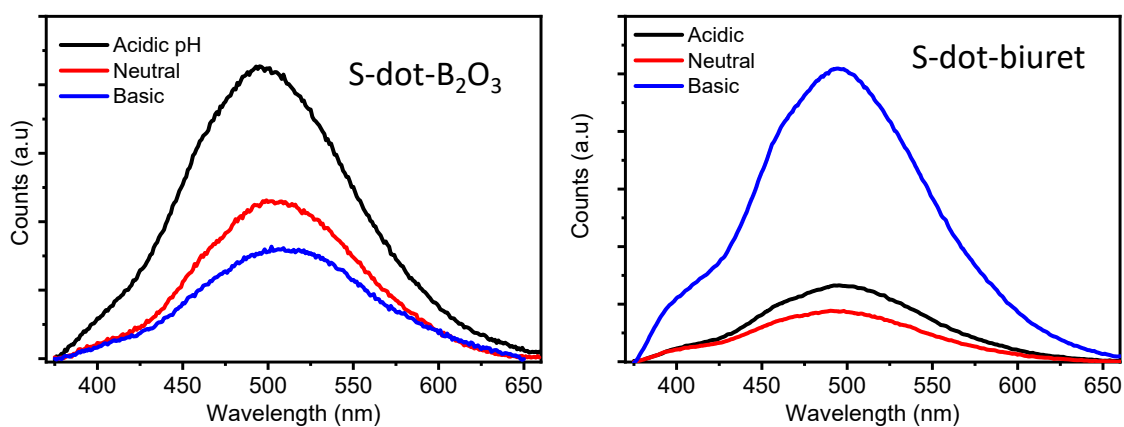
Figure S11. Phosphorescence spectra of S-dots embedded in various matrixes such as boron oxide and biuret matrix: S-dots in boron oxide matrix at various pH (acidic, neutral, and basic) and S-dots in biuret matrix at various pH (acidic, neutral, and basic).
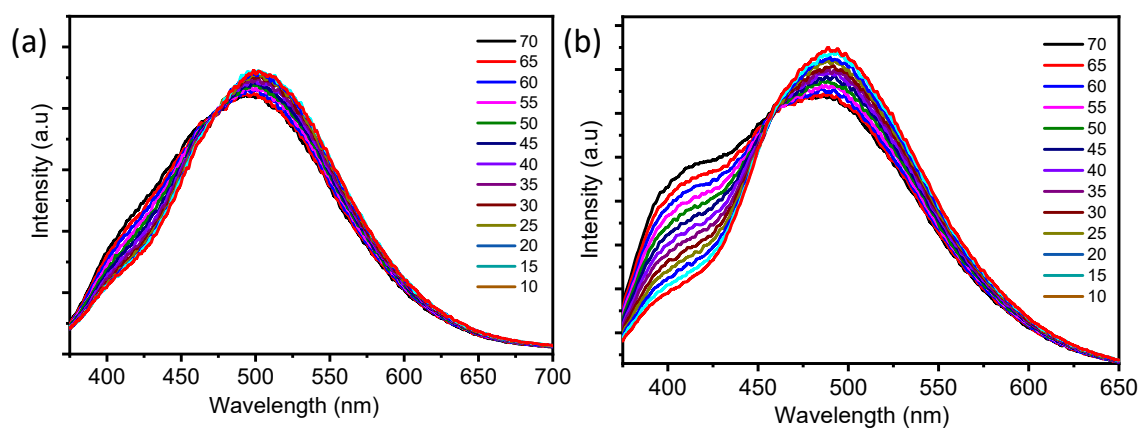
Figure S12. (a) Thermo-responsive phosphorescence spectra of S-dots/B_2O_3 composite by varying the temperature (cooling process) (b) thermo-responsive phosphorescence spectra of S-dots/biuret composite by varying the temperature (cooling process).

Table S2. Phosphorescence lifetime data of as-synthesized S-dots-B_2O_3 and S-dot-biuret composites at 365 nm excitation wavelength and heating (70 °C) and cooling (10 °C) processes.

Sample	Temperature		A_1	τ_1 (ms)	A_2	τ_2 (ms)	$<\tau>$ (ms)
S-dot-B_2O_3 composite	10 °C	RTP	0.45	48.820	0.54	602.77	351.85
	70 °C	RTP	0.62	49.090	0.37	463.1	204.34
S-dot-biuret composite	10 °C	RTP	0.47	53.930	0.53	549.43	316.54
	70 °C	RTP	0.59	38.030	0.41	418.84	194.15
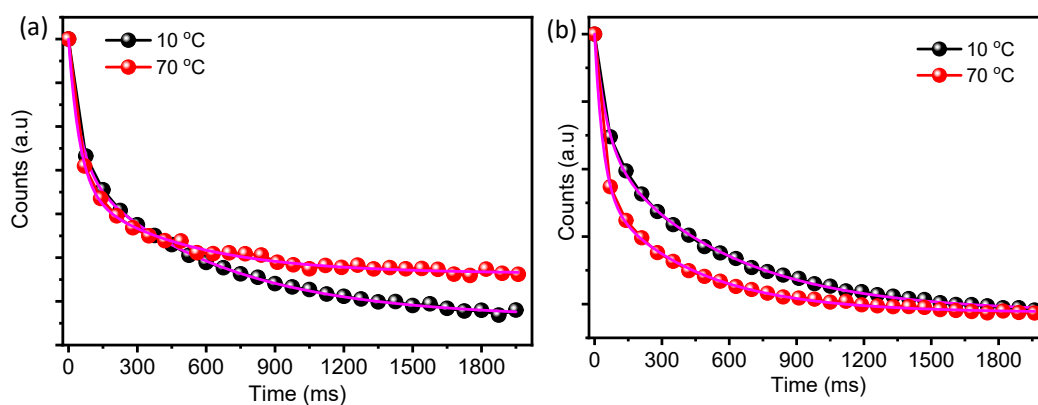
Figure S13. Phosphorescence lifetime data of S-dots in B_2O_3 and biuret matrix at heating (70 °C) and cooling (10 °C) process (a) phosphorescence lifetime data of S-dot/B_2O_3 composite (b) phosphorescence lifetime data of S-dot/biuret composite; fitted with biexponential decay kinetics.
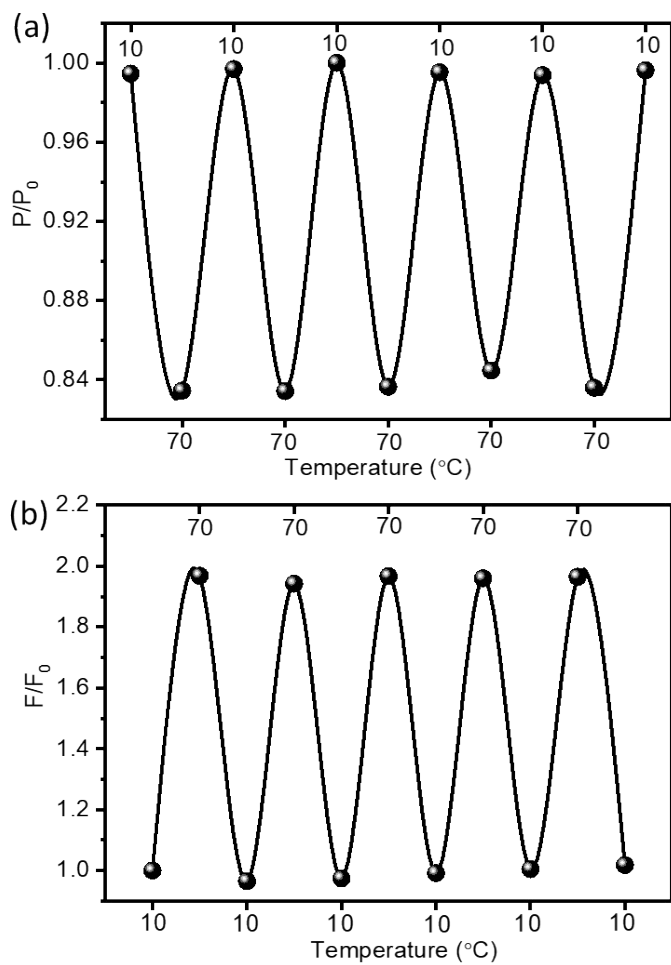
Figure S14. Temperature-dependent cycling stability plot for the (a) phosphorescence and (b) TADF of the S-dot-biuret composite at heating (70 °C) and cooling (10 °C) processes.